Original Article

DOI: 10.5582/bst.2025.01220

Neurotropin alleviates Alzheimer's disease pathology by inhibiting FUS-mediated Calhm2 transcription, blocking the Calhm2/EFhd2 interaction, to improve mitochondrial dysfunction-associated microglia polarization

Yuanlu Huang, Fusheng Wei, Xiaoe Cheng, Yinqi Shi, Ziye Liu, Lingling Ye*

Department of Anesthesiology and Operative Medicine, Medical Center of Anesthesiology and Pain, The First Affiliated Hospital of Nanchang University, Nanchang, Jiangxi, China.

SUMMARY: Neurotropin, a non-protein extract widely used for the treatment of neuropathic pain, has recently been reported to protect against ischemic brain injury, enhance remyelination in demyelinating diseases, and ameliorate neuroinflammation and memory deficits. However, its role in microglial polarization and mitochondrial dysfunction in Alzheimer's disease (AD) remains poorly understood. In this study, we investigated the therapeutic potential of Neurotropin in the 5xFAD mouse model of AD. Neurotropin administration alleviated cognitive decline, reduced amyloid-β (Aβ) deposition, suppressed neuroinflammation, and preserved neuronal density. Mechanistically, Neurotropin improved mitochondrial morphology, restored ATP production, increased mitochondrial DNA copy number, and reduced oxidative stress while promoting a shift in microglial polarization from the pro-inflammatory M1 phenotype toward the anti-inflammatory M2 phenotype. Transcriptomic and molecular analyses revealed that calcium homeostasis modulator family member 2 (Calhm2) was markedly upregulated in 5xFAD mice, colocalized with microglia, and transcriptionally regulated by fused in sarcoma (FUS), while Calhm2 interacted with EF-hand domain containing protein D2 (EFhd2). Neurotropin suppressed FUS-mediated Calhm2 transcription and attenuated Calhm2–EFhd2 interaction. Importantly, overexpression of Calhm2 in both microglial cells and 5xFAD mice abolished the beneficial effects of Neurotropin, leading to exacerbated mitochondrial dysfunction, oxidative stress, and inflammatory cytokine release. Together, these findings identify Calhm2 as a critical mediator of Neurotropin's neuroprotective effects and demonstrate that Neurotropin alleviates AD pathology by suppressing FUS-dependent Calhm2 transcription and blocking the Calhm2/EFhd2 interaction. This study provides new insights into the mechanism of Neurotropin action and highlights its therapeutic potential for AD.

Keywords: Neurotropin, Alzheimer's disease, FUS, Calhm2, EFhd2, mitochondrial dysfunction, microglia polarization

1. Introduction

Alzheimer's disease (AD) is a progressive neurodegenerative disorder and the leading cause of dementia worldwide (*1*). With the ongoing increase in the aging population, both the prevalence and incidence of AD continue to rise (*2*). By 2050, the number of individuals affected by dementia is projected to triple globally, placing an immense emotional and financial burden on patients, families, and healthcare systems (*3*). Clinically, AD is characterized by progressive memory loss, cognitive impairment, and behavioral disturbances (*4*). The main pathological hallmarks of AD include extracellular amyloid-beta (Aβ) plaques and intracellular neurofibrillary tangles composed of phosphorylated Tau protein (*5*). The intricate interaction between Aβ and Tau synergistically contributes to AD pathogenesis (*6*). Despite extensive efforts, clinical trials targeting Aβ or Tau alone have yielded limited success, underscoring the urgent need to identify and validate novel therapeutic targets for AD.

Neurotropin, an established analgesic derived from inflamed rabbit skin inoculated with the vaccinia virus, has been widely prescribed for the treatment of neuropathic pain in Japan and China for the past 50 years, with a well-documented safety profile (*7*). Beyond its analgesic effects, emerging evidence from animal studies suggests that Neurotropin also exerts notable neuroprotective properties (*8*). For example, three months of Neurotropin administration significantly improved spatial cognitive impairment in a Down syndrome mouse

model carrying triplication of 65% of human trisomy-21 genes (*8*). Despite these promising findings, research on Neurotropin in the context of AD remains scarce, and its potential therapeutic value and underlying mechanisms in AD have yet to be fully elucidated.

Microglia, the innate immune cells of the central nervous system (CNS), play a complex role in AD by mediating neuroinflammation, phagocytosis, and neurodegeneration (*9*). Upon activation, microglia can polarize into two major phenotypes: the pro-inflammatory M1 type, which releases cytokines that exacerbate neuronal damage, and the anti-inflammatory M2 type, which promotes repair and tissue homeostasis (*10*). Upon accumulation of Aβ plaques, microglia become excessively activated and secrete pro-inflammatory cytokines, including interleukin-1 beta (IL-1β), IL-6, and necrosis factor-alpha (TNF-α), thereby aggravating AD pathology (*11*). As AD progresses, the phagocytic capacity of microglia to clear Aβ plaques declines, resulting in increased plaque accumulation and disease progression (*12*). Furthermore, Aβ interacts with receptors of microglial cells, such as triggering receptors expressed in myeloid cells 2 (TREM2), initiating downstream pathways that cause mitochondrial injury and amplify cytotoxicity and inflammation, thereby accelerating AD progression (*13*). Based on these observations, we hypothesize that Neurotropin may attenuate M1-type microglial activation and protect against mitochondrial dysfunction in AD.

Calcium homeostasis is intricately connected to microglial activation. Recent research has increasingly focused on the role of calcium homeostasis modulator family proteins (Calhm), including Calhm1, Calhm2, and Calhm3, in AD (*14*). Calhm1, the most studied member, regulates calcium homeostasis, Aβ production, and neuronal vulnerability to Aβ-induced toxicity (*15*). The P86L mutation in Calhm1 is linked to a higher incidence of AD (*16*). Additionally, studies have shown that Calhm3 interacts with Calhm1, and the absence of Calhm3 abolishes taste-induced ATP release (*17*). Calhm2, highly expressed in the mouse brain, regulates ATP release in astrocytes (*14*). Loss of Calhm2 results in a depression-like phenotype in mice that significantly reduces Aβ deposition and neuroinflammation, and alleviates AD-related cognitive impairments (*14*). Our preliminary data indicated that Calhm2 expression was elevated in 5xFAD mice, whereas treatment with Neurotropin reduced Calhm2 expression in 5xFAD mice. These findings indicate that Calhm2 may play a critical role in mediating the therapeutic effects of Neurotropin in AZ.

Results from the bioinformatic prediction tool also suggest that fused in sarcoma (FUS) may potentially target Calhm2. FUS is an RNA/DNA-binding protein known to induce mitochondrial damage and mediate neurodegenerative pathogenesis (*18*). Additionally, FUS plays a critical role in stabilizing the mRNAs of its downstream target genes and can also function as a transcription factor (*19*). However, whether FUS participates in mediating microglial polarization and mitochondrial injury in AD and the underlying mechanism remains to be investigated.

Based on these findings, we hypothesize that Neurotropin alleviates AD by improving mitochondrial dysfunction and reducing microglial polarization through the inhibition of FUS-mediated transcriptional activation of Calhm2. This study may provide a theoretical basis for using Neurotropin as a treatment for AD.

2. Materials and Methods

2.1. Ethics statement

This research was conducted in strict accordance with the ARRIVE guidelines. The study protocol was thoroughly evaluated and received approval from the Ethics Committee of The First Affiliated Hospital of Nanchang University (Approval No. CDYFY-IACUC-202401QR002). To ensure humane treatment, mice were anesthetized using 3% isoflurane with oxygen as the carrier gas and subsequently euthanized with carbon dioxide.

2.2. Animal model of AD (5×FAD mice) and treatment

Five-month-old male 5xFAD transgenic (Tg) mice were purchased from Jackson Laboratory (stock no. 034848-JAX, Bar Harbor, ME, USA) and housed under a 12-hour light/12-hour dark cycle (lights on at 5:00 am) with free access to water and food; cages were cleaned weekly.

For the first experiment, 12 wildtype (WT, non-Tg) mice and 12 Tg mice were divided into four groups: non-Tg, non-Tg + Neurotropin, Tg, and Tg + Neurotropin (6 mice per group). Neurotropin (200 NU/kg, Nippon Zoki Pharmaceutical Co., Osaka, Japan) was administered orally using a Zonde needle daily from 5 to 7 months of age, while control groups received an equivalent volume of NaCl. At 8 months, these mice were also examined using behavioral tests for a continuous 5 days and were sacrificed. Afterward, the hippocampi from the mice were collected.

In the second experiment, 12 Tg mice were divided into Tg + Neurotropin + oe-NC and Tg + Neurotropin + oe-Calhm2 groups (6 mice each). Along with daily Neurotropin administration, stereotactic intracerebral injections of lentiviral particles (oe-NC or oe-Calhm2) were performed in month 6 of age based on a previously published protocol (*20*). Mice were anesthetized with 80 mg/kg ketamine hydrochloride and 5 mg/kg xylazine hydrochloride and fixed on a stereotactic frame. Lentiviral particles were injected into the cerebral cortex (anteroposterior = −0.3 mm, mediolateral = 2 mm, dorsoventral = −1.5 mm; anteroposterior = −2 mm, mediolateral = 1.2 mm, dorsoventral = −1.2 mm) and

hippocampi (anteroposterior = −2 mm, mediolateral = 1.2 mm, dorsoventral = −2 mm) using a micropipette attached to a 10-μL Hamilton syringe. At 8 months, these mice were also examined using behavioral tests for a continuous 5 days and were sacrificed. Afterward, hippocampi from the mice were collected. Hippocampi from 3 mice of each group were used for histological staining. The left hippocampi from 3 mice were reserved for transmission electron microscopy (TEM), and the right hippocampi were kept for other analyses. The detailed study design is summarized in Chart 1 of Supplementary materials (*https://www.biosciencetrends.com/action/getSupplementalData.php?ID=272*).

2.3. Morris water maze

Hippocampal-dependent memory and cognitive abilities were evaluated using established procedures. Mice were placed in a circular swimming pool with an 81 cm diameter, filled with water maintained at 24-25°C. An escape platform, 10 cm in diameter, was positioned 0.5 cm beneath the water's surface in the center of one quadrant. During the acquisition phase, mice were individually released into the water from random starting points along the pool wall in each of the four quadrants. This process was repeated four times daily for five consecutive days. Each trial allowed a maximum of 90 seconds for the mouse to locate the hidden platform. Once the platform was found, the mouse was allowed to remain on it for 15 seconds. If the mouse failed to find the platform within 90 seconds, it was guided to the platform by an experimenter. The time taken to reach the platform (escape latency) was recorded, with a maximum limit of 90 seconds. Swimming speed and the number of times the mice crossed the previous platform location were also recorded and analyzed using ANY-maze behavioral tracking software (Stoelting Co., Wood Dale, IL, USA).

2.4. Immunohistochemistry (IHC) staining.

Hippocampi were post-fixed in 4% paraformaldehyde for 24 hours, then paraffin-embedded and sectioned at a thickness of 4 μm. Sections were rehydrated through xylene and graded ethanol, treated with 3% hydrogen peroxide, and blocked with 10% normal goat serum for 45 minutes at room temperature. Amyloid deposits were detected using an anti-β-Amyloid 1-16 antibody (# SIG-39155, 1:1000, Biolegend, San Diego, CA, USA). Before antibody incubation, hippocampal sections were pre-incubated with 70% formic acid at 4°C for 24 hours, then rinsed in PBS. The sections were then incubated with a biotinylated anti-mouse IgG1 antibody (#ab97240, 1:250, Abcam, Cambridge, UK) for 90 minutes at room temperature. Following washes in PBS, sections were treated with DAPI for 10 minutes. Finally, sections were coverslipped with permanent mounting medium (Vector Laboratories, Burlingame, CA, US). All stained sections were observed and photographed under a microscope (Eclipse Ni-U, Nikon Instruments Inc., Tokyo, Japan), and areas of Aβ1-42 staining were quantified using Image Pro Plus 6.0.

2.5. Immunofluorescence (IF) staining

Hippocampal sections were rehydrated, treated, and blocked as previously described. Slides were then incubated overnight at 4°C with one of the following primary antibodies: anti-neuronal nuclei (NeuN, ab177487, 1:100; Abcam), anti-ionized calcium-binding adapter molecule 1 (Iba-1, ab178846, 1:1000; Abcam), anti-CD16/32 (45-0161-82, 1:1000; Thermo Fisher Scientific), anti-Arginase 1 (Arg1, 711765, 1:1000; Thermo Fisher Scientific), anti-Calhm2 (19931-1-AP, 1:200; Proteintech), or anti- EF-hand domain-containing protein D2 (EFhd2, PA5-78575, 1:500; Thermo Fisher Scientific). The following day, sections were washed three times with PBS and then incubated with secondary antibodies (Abcam) for 2 hours at room temperature. Nuclear staining was performed using DAPI (Life Technologies, Waltham, CA, USA). Fluorescently labeled cells were visualized using an LSM 710 ZEISS microscope (Jena, Germany). Ten images per sample were captured and quantified using ImageJ.

2.6. Enzyme-linked immunosorbent assay (ELISA) assay

ELISA kits (ab108865, ab100713, and ab108910 from Abcam) were utilized to measure expression levels of IL-1β, IL-6, and TNF-α in serum and hippocampal tissues, according to the manufacturer's instructions. Regarding hippocampus tissue, they were homogenized in a mixture of phenylmethylsulfonyl fluoride (PMSF) and radioimmunoprecipitation assay (RIPA) lysis buffer (Solarbio Science & Technology Co., Ltd., Beijing, China) at a ratio of 10 μL PMSF to 1 mL RIPA lysis buffer, kept on ice. The homogenates were centrifuged at 12,000 rpm for 5 minutes at 4°C, and supernatant protein concentrations were determined using a BCA Protein Assay kit (Beyotime Institute of Biotechnology, Shanghai, China). For each sample, 5 μL of extracted protein was used for detection. Absorbance was measured at 450 nm using a spectrophotometer, and concentrations were calculated using a standard curve.

2.7. TEM

The CA1 region of the left hippocampus was carefully dissected and fixed in 3% buffered glutaraldehyde. This was followed by post-fixation in 1% osmium tetroxide. The samples were then dehydrated using a series of increasing ethanol concentrations and embedded in Epon 812. The ultrastructure of the hippocampal CA1 subregion was visualized with a TEM (Philips,

Amsterdam, Netherlands). Images were taken from five randomly selected sections. These images were analyzed for morphometric parameters using Image Pro Plus 6.0. Stereological methods used for analyzing synapses and mitochondria were as previously described. Measurements included mitochondrial length (mito length)/mitochondrial width and copy number of mitochondrial DNA (mtDNA).

2.8. Mitochondrial membrane potential (MMP) assay

A mitochondrial membrane potential assay kit with 5,5′,6,6′-tetrachloro-1,1′,3,3′-tetraethylbenzimidazolyl-carbocyanine iodide (JC-1) (C2006; Beyotime Institute of Biotechnology) was used to detect MMP. JC-1 accumulates in mitochondria with higher membrane potentials, forming J-aggregates that emit red fluorescence (Cy3, excitation/emission wavelength of 525/590 nm). In mitochondria with lower membrane potentials, JC-1 remains in monomeric form, emitting green fluorescence (fluorescein isothiocyanate [FITC], excitation/emission wavelength of 490/530 nm). A decrease in the red: green fluorescence ratio indicates a decrease in MMP. For this assay, 0.1 mL of purified mitochondria (protein concentration 0.2 mg/mL) from different groups were incubated with 0.9 mL of 0.2X JC-1 staining working solution. A time scan was performed using a fluorescence microplate reader (Gemini EM Microplate Reader, Molecular Devices, Sunnyvale, CA, USA) with an excitation/emission wavelength of 485/590 nm and observed under an Olympus BX5 fluorescence microscope imaging system (Olympus America, Melville, NY, USA).

2.9. Malondialdehyde (MDA) and superoxide dismutase (SOD) measurement

MDA is a byproduct of lipid peroxidation and serves as a reliable indicator of oxidative stress. Levels of MDA in the hippocampi of mice were measured using commercial assay kits from Beyotime Biotechnology Institute (S0131S) following the manufacturer's instructions. The measurement is based on reaction of one molecule of MDA with two molecules of thiobarbituric acid, yielding a pink-colored chromogen. Color intensity was measured at 532 nm, with a reference wavelength of 450 nm. The activity of SOD in hippocampus tissue samples was measured using commercial assay kits from Beyotime Biotechnology Institute (S0086), according to the manufacturer's instructions. The assay involves the reaction of nitroblue tetrazolium with superoxide anion, producing a blue-colored chromogen.

2.10. ATP content and activity of the respiratory chain complex I

ATP content of hippocampal tissues was measured using the Enhanced ATP Assay Kit (S0027, Beyotime Biotechnology) and the Electron Transport Chain Complex I Assay Kit (S0026, Beyotime Biotechnology), following the manufacturer's instructions. Results are presented as fold-change values relative to the control group (non-Tg mice).

2.11. Cell culture, treatment, and transfection

Mouse microglia BV2 cells were obtained from the American Type Culture Collection (ATCC) and routinely cultured in Dulbecco's Modified Eagle's Medium (DMEM) supplemented with 10% fetal bovine serum (FBS) and penicillin/streptomycin (Gibco, Carlsbad, CA) in 6 cm plates. BV-2 cells were seeded in 6-well plates at a density of 1×10^5 cells per well for 24 hours. Cells were then treated with or without Neurotropin (0.1 NU/mL) for 12 hours before being exposed to lipopolysaccharide (LPS, 100 ng/mL, L2630, Sigma-Aldrich, St Louis, MO, USA) for an additional 12 hours. Cells were plated 24 hours before transfection at 70-80% confluency. Custom-designed small interfering RNA (siRNA) targeting FUS (si-FUS) and control siRNA (si-NC) were provided by Genesee Biotech and integrated into pCD513B-U6 plasmids by Genepharma (Shanghai, China) to construct siRNA vectors. For Calhm2 overexpression, the full-length Calhm2 sequence was amplified by PCR and cloned into pcDNA3.1 plasmids obtained from SBI (Mountain View, CA, USA). Empty plasmids were used as negative controls. Calhm2 overexpression transfection was carried out using Lipofectamine 3000 reagent according to the manufacturer's protocol. The small RNA interference transfection was performed using Lipofectamine RNAiMAX (Invitrogen, Carlsbad, CA) following the manufacturer's instructions.

2.12. Mitochondrial reactive oxygen species (mtROS) production assay

To measure mitochondrial superoxide levels, cells were incubated with MitoSOX™ Red Mitochondrial Superoxide Indicator (11579096, Invitrogen, Ltd., UK) at 30°C for 10 minutes, then washed three times with PBS. SOD was added at a concentration of 40 U/mL as a negative control for superoxide after the MitoSOX™ Red treatment. Levels of mtROS were analyzed using a BD FACSCalibur (BD Biosciences, San Jose, CA, USA).

2.13. RNA extraction and quantitative real-time polymerase chain reaction (RT-qPCR)

Total RNA was isolated using Trizol reagent (15596026, Invitrogen). One microgram of RNA was reverse transcribed into cDNA using the PrimeScript cDNA synthesis kit (6110A, Takara, Osaka, Japan) following the manufacturer's instructions. Quantitative PCR was then performed using the TaqMan® Universal PCR Master

Mix (4305719, Thermo Fisher Scientific, Waltham, MA, USA) and primers from Origen Biotech (Wuxi, Jiangsu, China), as listed in Supplementary Table S1 (*https://www.biosciencetrends.com/action/getSupplementalData.php?ID=272*). Relative mRNA levels were calculated using the $2^{-\Delta\Delta Ct}$ method and normalized to GAPDH expression.

2.14. Western blot

Proteins were extracted using radio-immunoprecipitation assay (RIPA) buffer supplemented with protease inhibitors at 4°C for 30 minutes (Beyotime Inc.). Protein concentrations were determined using a bicinchoninic acid (BCA) protein assay kit (10741395, Thermo Fisher Scientific). For each sample, 30 μg of protein was separated by sodium dodecyl sulfate–polyacrylamide gel electrophoresis (SDS-PAGE) and transferred onto polyvinylidene fluoride (PVDF) membranes (Merck Millipore). Membranes were blocked and rinsed with PBS before being incubated with primary antibodies against Calhm2 (PA5-53219, 1:10,000, Thermo Fisher Scientific), EFhd2 (PA5-78575, 1:1,000, Thermo Fisher Scientific), FUS (PA5-52610, 1:1,000, Thermo Fisher Scientific), and β-catenin (13-8400, 1:200, Thermo Fisher Scientific). After additional PBS washing, the membranes were incubated with secondary antibodies (31402, 1:2,000, Invitrogen) and visualized using an ECL kit (WBULS0100, Merck Millipore, MA, USA).

2.15. Chromatin immunoprecipitation (ChIP) assay

BV2 cells were harvested and lysed with RIP lysis buffer (Merck Millipore). Following cell cross-linking and sonication, samples were supplemented with 20 μL of 50× protease inhibitor cocktail (PIC), 900 μL of ChIP Dilution Buffer, 20 μL of 50× PIC, and 60 μL of Protein A Agarose/Salmon Sperm DNA. After incubation, the samples were centrifuged, and the supernatant was carefully transferred to a new tube. Next, 1 μL of anti-FUS antibody (11570-1-AP, 1:200, Thermo Fisher Scientific) or IgG antibody (ab181569, 1:50, Abcam) was added to the supernatant and incubated overnight at 4°C. Following precipitation and washing steps, 1 μL of RNase A was added to each tube and incubated at 37°C for 1 hour. Subsequently, 10 μL of 0.5 M EDTA, 20 μL of 1 M Tris-HCl, and 2 μL of 10 mg/mL proteinase K were added to each tube and incubated at 45°C for 2 hours. Finally, DNA samples were collected and quantified using qPCR.

2.16. Dual-luciferase reporter assay

The experimental protocol followed the procedures outlined in a previously published study. Briefly, BV-2 cells were transfected with si-FUS or si-NC using Lipofectamine 3000 transfection reagent (Invitrogen). After 48 hours of incubation, luciferase activities were measured using the Dual-Luciferase Reporter Assay Kit (Promega, Shanghai, China) to assess the luciferase activity of Calhm2.

2.17. Co-immunoprecipitation (Co-IP) assay

Hippocampal tissues were washed twice with PBS, followed by treatment using a buffer containing 50 mM NaCl (pH 7.4), 1 mM EDTA, 1 mM EGTA, and 0.05% Triton X-100. Resulting lysates were sonicated on ice in an IP buffer and centrifuged at 12,000 rpm for 10 minutes. A 30 μL aliquot of the supernatant was collected as the input sample. Additionally, 420 μL of the supernatant underwent overnight immunoprecipitation at 4°C with an anti-HA-tag-Calhm2 antibody (customized by Thermo Fisher Scientific) or a control nonspecific IgG antibody (1:1000, ab18413, Abcam). Protein A was then added and incubated for 1 hour at 4°C. After four washes with IP buffer, the samples were centrifuged for 2 minutes, and the supernatant was discarded. Finally, 30 μL of 2X SDS sample buffer was added and incubated for 10 minutes. The samples were then subjected to immunoblotting.

2.18. Statistical analysis

Data analysis was conducted using GraphPad Prism 5.0 software (GraphPad Software, Inc., CA, USA). Data are presented as the mean ± standard deviation (SD) from at least three independent experiments. An unpaired Student's *t*-test was used to assess differences between the two groups. For comparisons involving more than two groups, a one-way analysis of variance (ANOVA) was initially performed, except for MVM test data, which was analyzed using two-way ANOVA. This was followed by the Tukey post hoc test for further analysis. Statistical significance was defined as $P < 0.05$.

3. Results

3.1. Neurotropin ameliorated Aβ pathology and cognitive decline in 5xFAD mice

To elucidate the effect of Neurotropin in AD, 5xFAD transgenic (Tg) mice and WT (non-Tg) controls were administered Neurotropin. In non-Tg mice, Neurotropin treatment did not alter escape latency, swimming speed, or the number of target quadrant crossings during the probe trial (Figure 1A-1C). In contrast, Tg mice exhibited markedly longer escape latency, faster swimming speed, and fewer target quadrant crossings compared to non-Tg mice. Importantly, Neurotropin treatment significantly attenuated these deficits, indicating a protective effect on cognitive performance. To further assess pathology, IHC staining was performed to evaluate amyloid plaque burden in the hippocampus. As expected, no plaques

were detected in the hippocampus of non-Tg mice, regardless of treatment (Figure 1D). By contrast, Tg mice displayed a substantial increase in hippocampal plaques, which was significantly reduced by Neurotropin treatment. These results collectively indicate that Neurotropin alleviated Aβ pathology and associated cognitive decline in 5xFAD mice.

Building on these findings, we next investigated whether Neurotropin modulates microglial activation and neuroinflammation in Tg mice. IF staining for NeuN (neuronal marker) and Iba-1 (microglial marker) was performed on hippocampal sections. No differences in neuronal density or microglial activation were observed in non-Tg mice, regardless of treatment (Figure 1E–1F). However, Tg mice exhibited neuronal loss and increased Iba-1 immunoreactivity, indicative of microglial activation and neuronal damage, which were ameliorated by Neurotropin treatment. Furthermore, analysis of inflammatory cytokines revealed no significant changes in IL-1β, IL-6, and TNF-α levels in either the serum or hippocampal tissues of non-Tg mice with or without treatment (Figure 1G-1H). In Tg mice, these pro-inflammatory markers were significantly elevated, and this elevation was notably suppressed by Neurotropin administration. Taken together, Neurotropin not only reduced Aβ pathology but also mitigated neuroinflammation and microglial activation in 5xFAD mice, further supporting its therapeutic potential in AD.

3.2. Neurotropin improved impaired mitochondrial dysfunction, repressed oxidative stress, and alleviated energy crises in 5xFAD mice

Given that mitochondrial dysfunction is closely linked

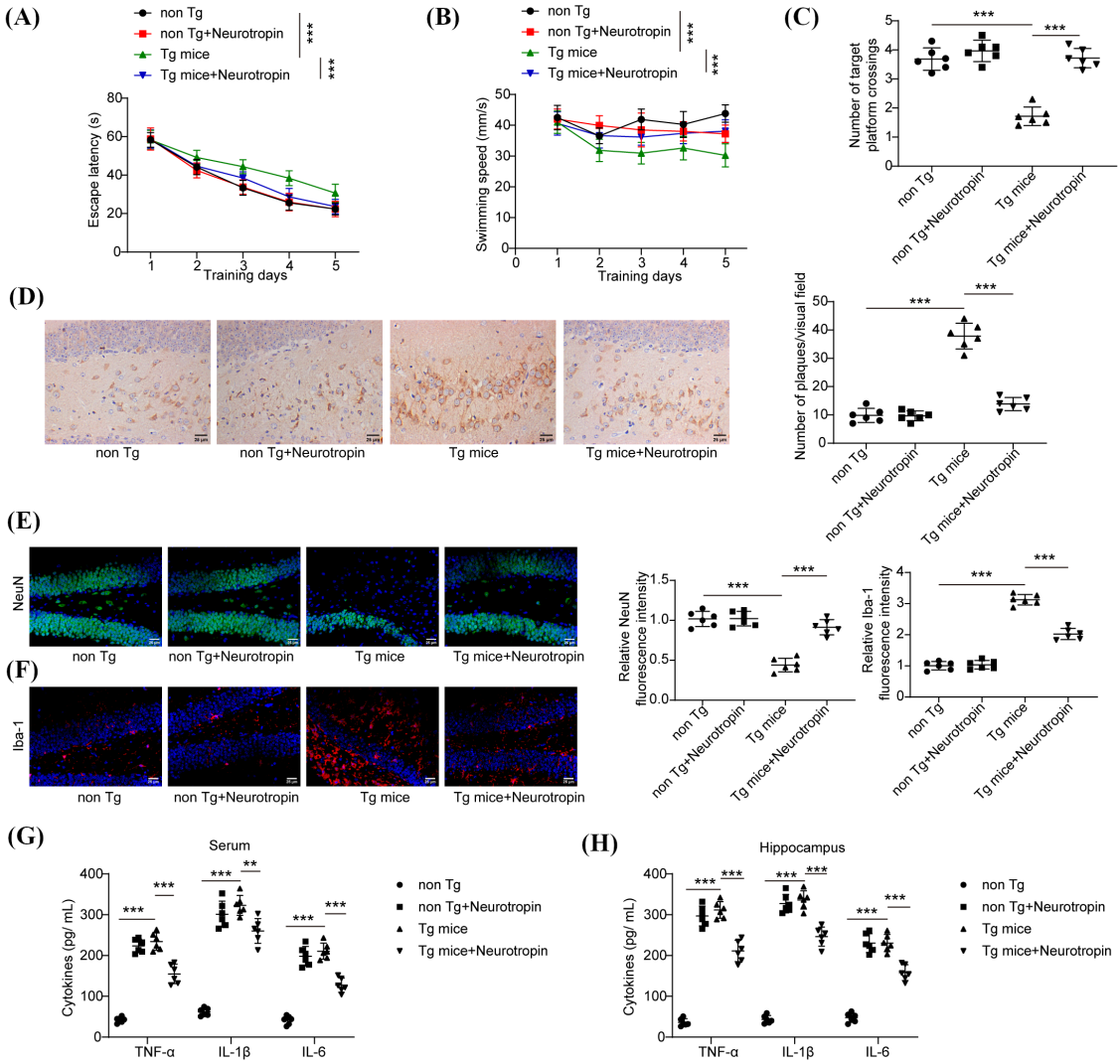

Figure 1. Neurotropin ameliorates Aβ pathology and cognitive decline in 5xFAD mice. WT mice (non-Tg) or 5xFAD mice (Tg mice) were treated without or with Neurotropin. **(A)** Escape latency and **(B)** swimming speed during 5 days of hidden platform tests were measured. **(C)** Crossings of the target quadrant during the probe trial were measured. **(D)** Immunohistochemical staining of 6E10 in the hippocampus of mice, and the number of plaques was quantified. **(E)** Neuronal cell damage in hippocampal sections was detected by IF staining. **(F)** Iba-1-positive cells in hippocampal sections were detected by IF staining. IL-1β, IL-6, and TNF-α levels in **(G)** serum and **(H)** hippocampal tissues were measured using ELISA assays. $n = 6$. $^{**}p < 0.01$, $^{***}p < 0.001$.

to AD pathology (*21*), we next examined whether Neurotropin influences mitochondrial homeostasis. As expected, the mitochondrial length/width ratio and the copy number of mtDNA in the hippocampus were significantly decreased in Tg mice compared to non-Tg mice (Figure 2A-2B). Similarly, hippocampal ATP levels and respiratory chain complex I activity were markedly decreased in Tg mice but significantly restored by Neurotropin (Figure 2C-2D). In addition, Tg mice showed elevated oxidative stress, as indicated by increased MDA production and reduced SOD activity (Figure 2E-2F), both of which were ameliorated by Neurotropin. Altogether, Neurotropin protected against mitochondrial dysfunction, oxidative stress, and bioenergetic deficits in 5xFAD mice.

3.3. Neurotropin suppressed LPS-induced M1 microglia polarization but promoted microglia polarization to the M2 phenotype of microglia

We next investigated whether Neurotropin regulates microglial polarization. In the hippocampus of non-Tg mice, LPS treatment increased the proportion of CD16/CD32 (M1 marker)/Iba1 cells without affecting the proportion of Arg (M2 marker)/Iba1 cells, irrespective of Neurotropin administration (Figure 3A-3D). In contrast, Tg mice exhibited a significant reduction in CD16/CD32/Iba1 cells and an increase in Arg/Iba1 cells following Neurotropin treatment. Consistent with these results, Neurotropin reduced hippocampal gene expression of iNOS and CD86, as well as iNOS protein levels, while enhancing Arg and TGFβ1 gene expression and Arg1 protein levels (Figure 3E-3F). These findings suggest that Neurotropin suppressed M1 microglial polarization and promoted a shift toward the M2 phenotype in Tg mice.

3.4. Calhm2 overexpression reversed neurotropin's protective effects against LPS-induced microglial inflammation and mitochondrial stress

The underlying mechanism of Neurotropin-mediated effects in AD was also explored. No significant differences in Calhm1 expression were detected among

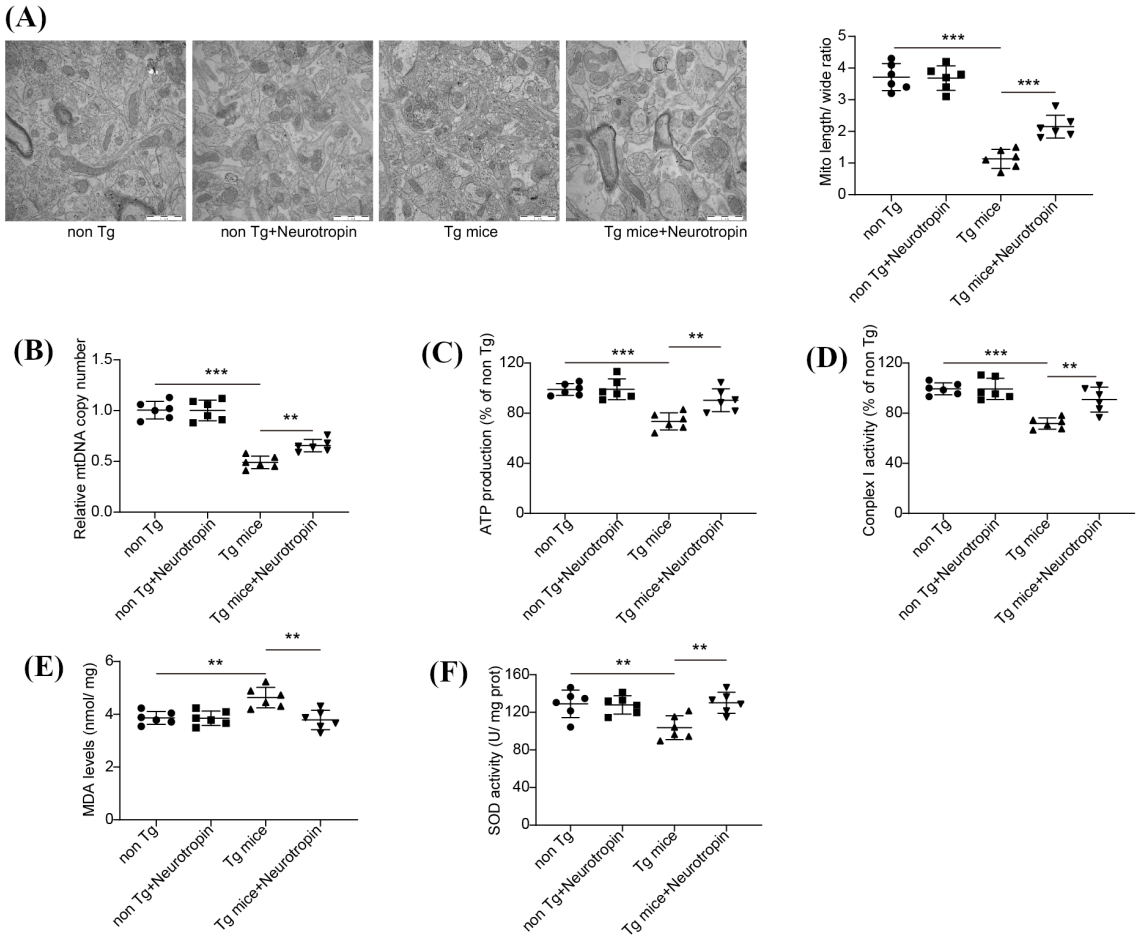

Figure 2. Neurotropin improved impaired mitochondrial dysfunction, repressed oxidative stress, and alleviated energy crisis in 5xFAD mice. WT mice (non-Tg) or 5xFAD mice (Tg mice) were treated without or with Neurotropin. **(A)** The morphology of mitochondria in the hippocampus was observed by TEM. **(B)** The copy number of mitochondrial DNA (mtDNA) in the hippocampus was measured. Energy metabolism was estimated based on **(C)** ATP levels and **(D)** respiratory chain complex I activity in the hippocampus. **(E)** MDA production and **(F)** SOD activity were assessed. $n = 6$. $^{**}p < 0.01$, $^{***}p < 0.001$.

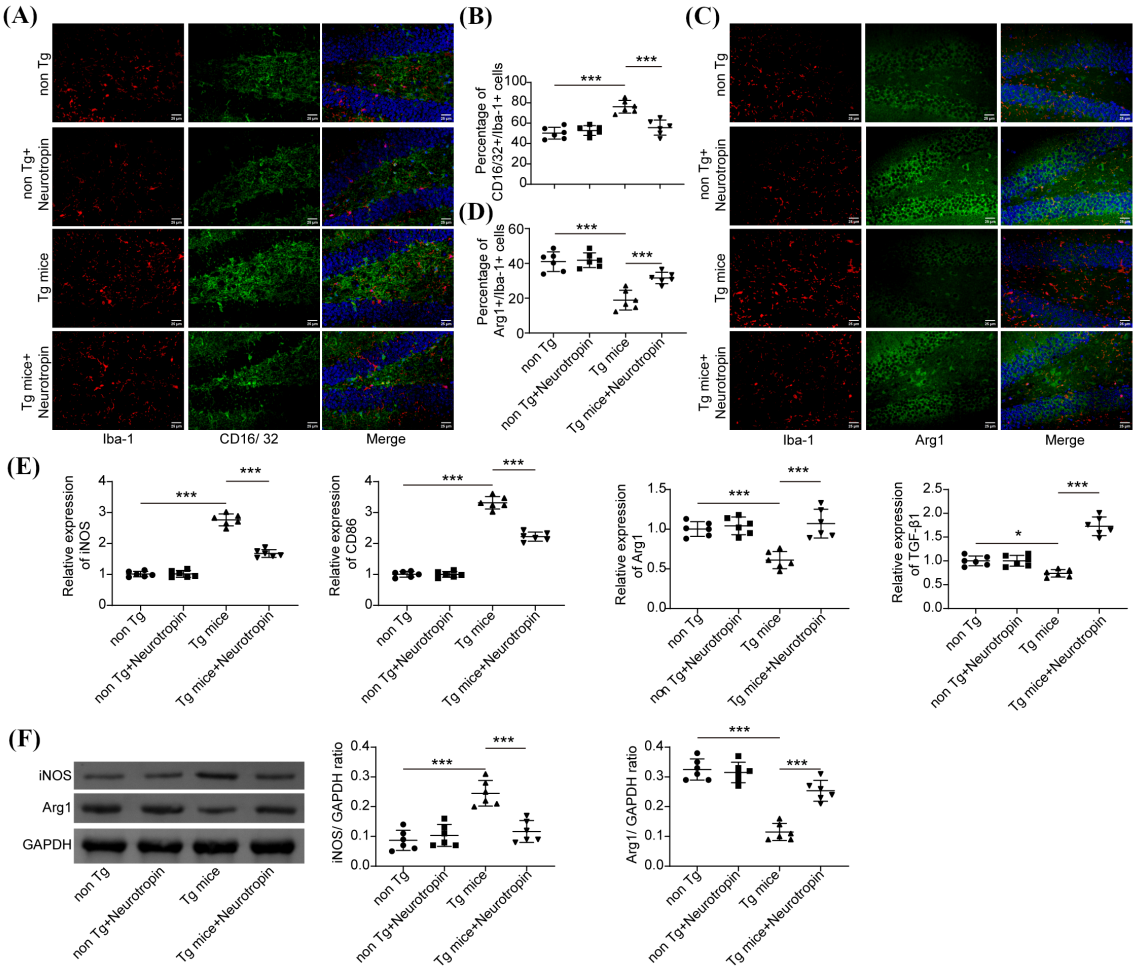

Figure 3. Neurotropin suppressed LPS-induced M1 microglia polarization but promoted microglia polarization to the M2 phenotype of microglia. WT mice (non-Tg) or 5xFAD mice (Tg mice) were treated without or with Neurotropin. Co-expression of Iba1 and the M1 polarization marker, CD16/32, in hippocampal sections was assessed by IF staining **(A)**, and the quantitative results were calculated based on the images **(B)**. Co-expression of Iba1 and the M2 polarization marker, Arg1, in hippocampal sections was assessed by IF staining, and **(C)** the quantitative results were calculated based on the images **(D)**. **(E)** Gene expression of iNOS, CD86, Arg1, and TGFβ1 in hippocampal sections was measured by qRT-PCR assay. **(F)** Protein expression of iNOS and Arg1 in hippocampal sections was measured by Western blot analysis. $n = 6$, $^{*}p < 0.05$, $^{***}p < 0.001$.

non-Tg or Tg mice treated without or with Neurotropin (Figure 4A). However, Calhm2 and Calhm3 expression levels were significantly increased in Tg mice compared to non-Tg mice. Neurotropin treatment in Tg mice significantly attenuated Calhm2 expression but did not significantly alter Calhm3 expression, indicating that Calhm2 may play a specific role in the response to Neurotropin treatment in Tg mice. Western blot analysis confirmed that Calhm2 protein expression was elevated in Tg mice but suppressed following Neurotropin treatment (Figure 4B). Additionally, Calhm2 was found to be colocalized with Iba-1. These findings suggest that Calhm2 may serve as a regulatory node in the therapeutic effect of Neurotropin in Tg mice.

To validate the role of Calhm2 in these processes, Calhm2 was overexpressed in LPS/Neurotropin-treated BV-2 cells. Neurotropin mitigated the promotional effect of LPS treatment on pro-inflammatory cytokine excretion, including IL-1β, IL-6, and TNF-α, in BV-2 cells, while Calhm2 overexpression reversed the effects of Neurotropin treatment (Figure 5A). The LPS-induced mtROS levels and JC-1 expression were suppressed by Neurotropin treatment in BV-2 cells (Figure 5B-5E). However, the overexpression of Calhm2 had the opposite effect. Neurotropin treatment reduced the quantity of $CD16/CD32^{+}$ cells, which were induced by LPS, in BV-2 cells (Figure 5F). Nevertheless, Calhm2 overexpression led to a further increase in $CD16/CD32^{+}$ cells in LPS/Neurotropin-treated BV-2 cells. Additionally, the expression of Calhm2 was enhanced by LPS treatment but suppressed upon Neurotropin treatment (Figure 5G). After Calhm2 overexpression, the expression of Calhm2 was again increased. These results indicate that Calhm2 mediated Neurotropin's anti-inflammatory and mitochondrial protective effects in microglia.

3.5. Neurotropin suppressed FUS-mediated Calhm2 transcription and disrupted Calhm2–EFhd2 interaction

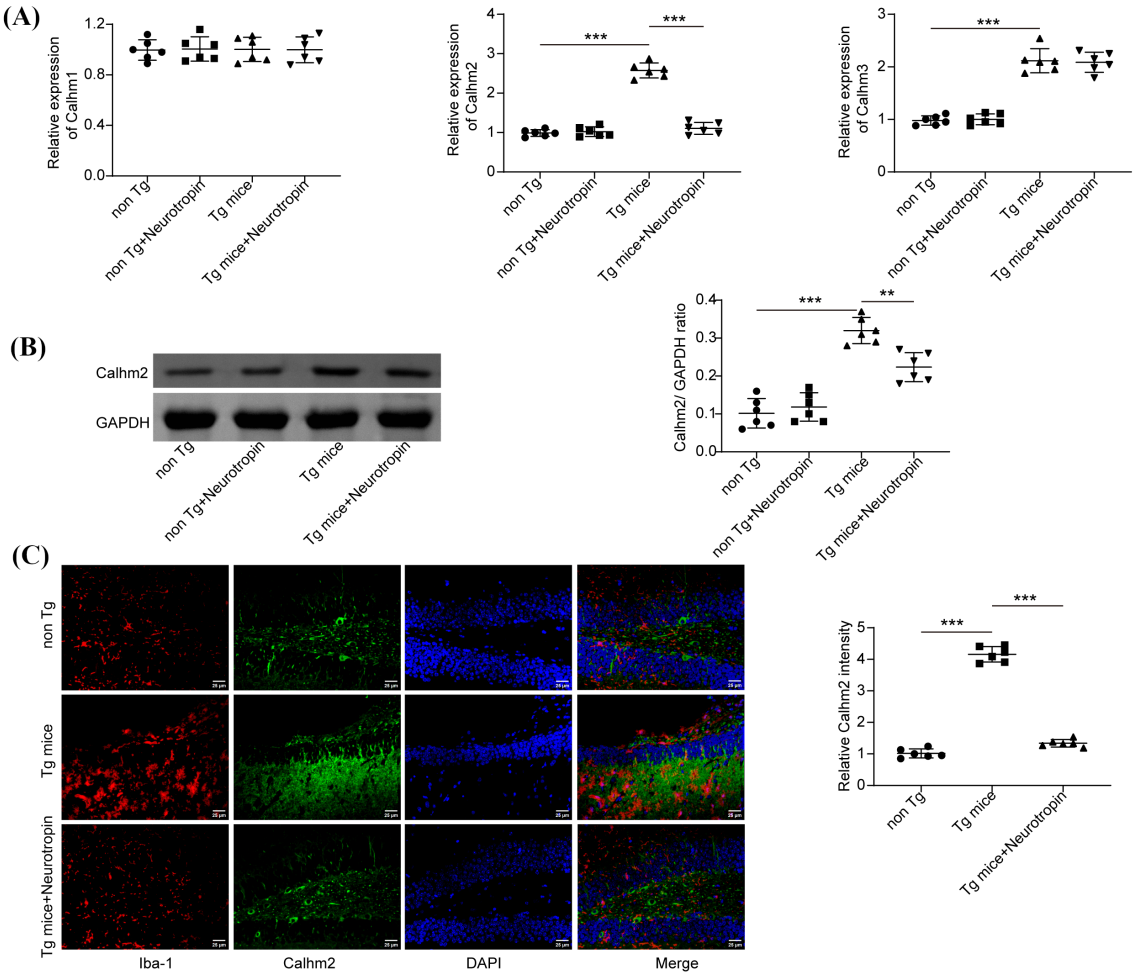

Figure 4. Calhm2 may play a role in Neurotropin treatment. WT mice (non-Tg) or 5xFAD mice (Tg mice) were treated without or with Neurotropin. **(A)** Gene expression of Calhm1, Calhm2, and Calhm3 was detected by qRT-PCR analysis. **(B)** Protein expression of Calhm2 was assessed by Western blot analysis. **(C)** Co-localization of Calhm2 and Iba-1 was examined by immunofluorescence staining. $n = 6$, $^{**}p < 0.01$, $^{***}p < 0.001$.

To explore the upstream regulation of Calhm2, we utilized bioinformatic tools. RNA-society predicted that FUS might potentially bind to Calhm2 (Figure 6A; last accessed October 2023). JASPAR provided the DNA motif for FUS binding (Figure 6B; last accessed October 2023). Calhm2 was significantly enriched when treated with antibodies against FUS (Figure 6C). Additionally, the relative luciferase activity of Calhm2 was markedly increased in cells transfected with si-FUS (Figure 6D). Knockdown of FUS significantly reduced the expression levels of both FUS and Calhm2 (Figure 6E). FUS protein levels were elevated in Tg mice compared to non-Tg and Neurotropin-treated non-Tg mice (Figure 6F). In contrast, Neurotropin treatment led to a decrease in FUS protein levels in Tg mice. Altogether, FUS targeted Calhm2 to mediate its transcription.

Subsequently, to investigate the regulatory mechanism of Calhm2, we performed Co-IP analysis using an immunoprecipitated Flag-Calhm2 antibody from cell lysates to identify potential interacting proteins, specifically EFhd2. Co-IP verified that Calhm2 interacted with EFhd2 in brain tissue from mice (Figure 6G). Additionally, Neurotropin treatment reduced the interaction between Calhm2 and EFhd2. Further analysis revealed that Calhm2 and EFhd2 were colocalized in the cytoplasm of LPS-treated BV-2 cells, and their fluorescence intensities were significantly reduced upon Neurotropin treatment (Figure 6H). Overexpression of Calhm2 did not significantly impact EFhd2 mRNA and protein expression levels (Figure 6I-6J). These data indicate that while Calhm2 interacted with EFhd2, it did not regulate its mRNA and protein expression.

3.6. Neurotropin rescues brain ATP deficiency, mitochondrial dysfunction, and microglia M1 polarization *via* Calhm2 in 5xFAD mice.

To validate the *in vitro* findings, we next investigated the role of Calhm2 *in vivo* using 5xFAD mice. Overexpression of Calhm2 significantly increased amyloid plaque burden in the hippocampus of Neurotropin-treated Tg mice (Figure 7A). Additionally,

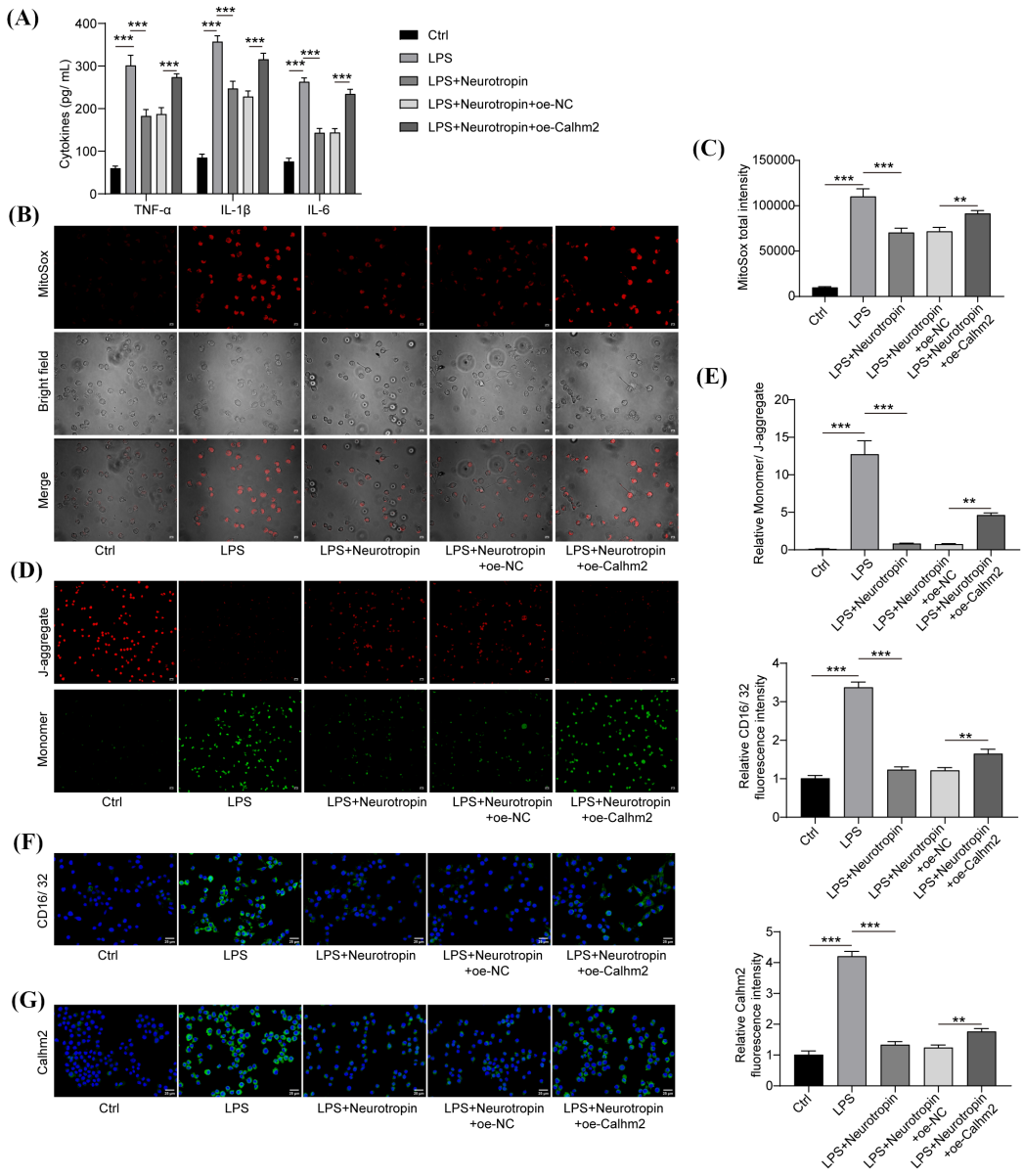

Figure 5. Calhm2 overexpression reversed neurotropin's protective effects against LPS-induced microglial inflammation and mitochondrial stress. Mouse-derived microglial BV-2 cells were treated without (control, ctrl) or with LPS, LPS/Neurotropin/oe-NC, or LPS/Neurotropin/oe-Calhm2. **(A)** ELISA assays were conducted to measure IL-1β, IL-6, and TNF-α. **(B)** Mitochondrial superoxide production was detected, and **(C)** quantitative analysis was performed to assess mitochondrial ROS (MitoSox, red). **(D)** Representative JC-1 IF staining images and **(E)** quantitative analysis. **(F)** Representative CD16/32 IF staining images and quantitative analysis. **(G)** Calhm2 was detected by immunofluorescence staining. $n = 3$, $^{**}p < 0.01$, $^{***}p < 0.001$.

Calhm2 was colocalized with Iba-1 in the hippocampus of Neurotropin-treated Tg mice (Figure 7B). The levels of IL-1β, IL-6, and TNF-α in both serum and hippocampal tissues were markedly elevated in Calhm2-overexpressing mice (Figure 7C-7D). Furthermore, Calhm2 overexpression resulted in reduced mitochondrial length-to-mitochondrial ratio, ATP levels, and respiratory chain complex I activity in the hippocampus (Figsure 7E-7F). MDA production, SOD activity, and CD16/32 fluorescent staining intensity were also significantly increased in Calhm2-overexpressing mice (Figure 7G-7H). Taken together, Neurotropin protected against brain ATP deficiency, mitochondrial dysfunction, and microglial polarization *via* Calhm2 in 5xFAD mice.

4. Discussion

Neurotropin is extensively utilized as an analgesic for treating intractable neuropathic pain (*22*). Recent research has revealed that Neurotropin can protect the brain from ischemic stroke, enhance remyelination in demyelinating diseases, and reduce memory impairment and neuroinflammation (*8,23*). However, its effects on microglial polarization and mitochondrial dysfunction in AD have yet to be investigated. This study demonstrated that Neurotropin inhibited microglia

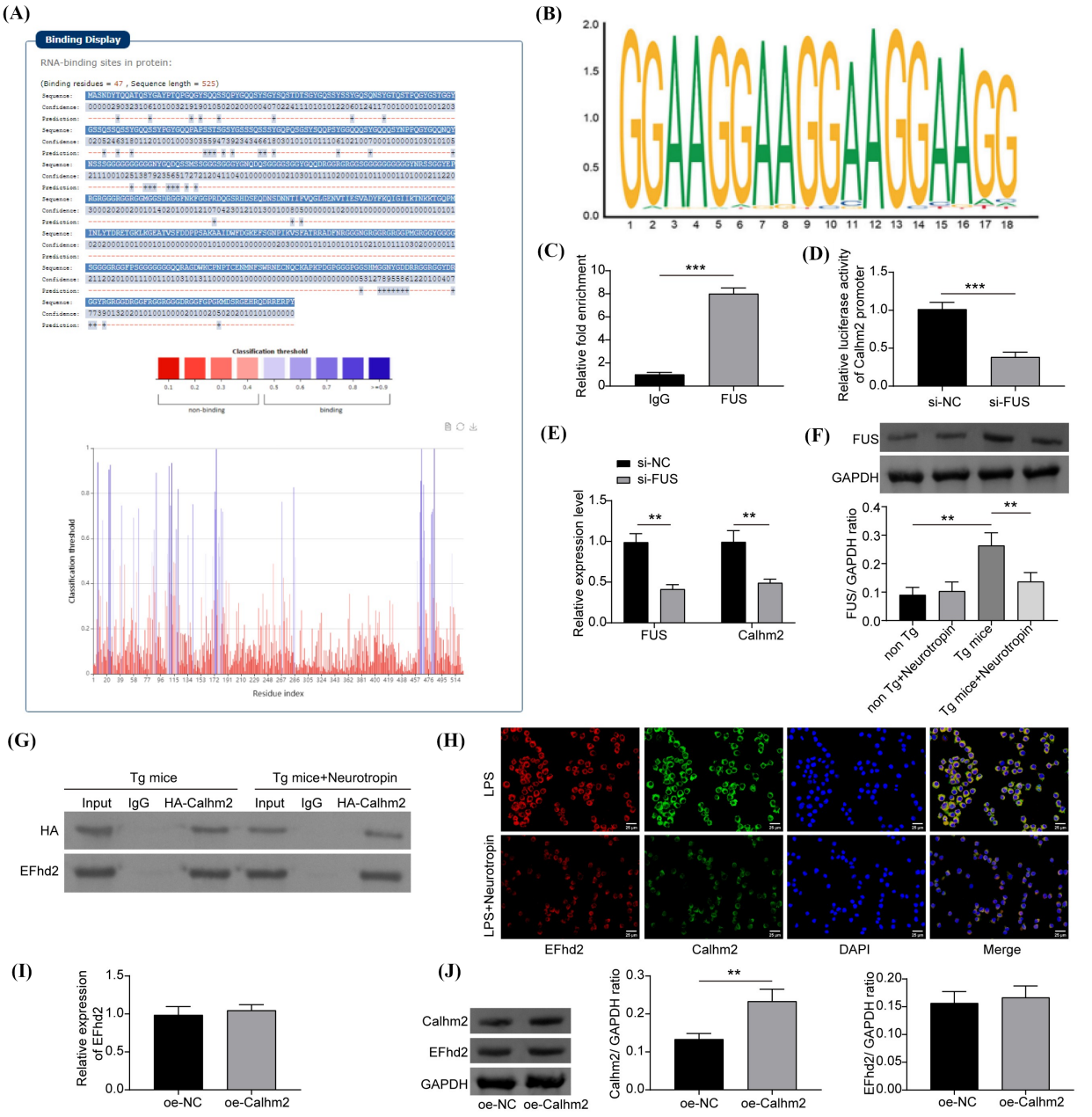

Figure 6. Neurotropin suppressed FUS-mediated Calhm2 transcription and disrupted Calhm2–EFhd2 interaction. (A) The potential binding relationship between FUS and Calhm2 was predicted using bioinformatics. **(B)** The DNA motif of FUS was obtained from JASPAR. The binding of FUS to the Calhm2 promoter was assessed by **(C)** ChIP and **(D)** luciferase reporter assays. **(E)** Calhm2 expression was detected by qRT-PCR. **(F)** *In vivo* levels (n=6) were assessed in WT mice (non-Tg mice), 5xFAD mice (Tg mice), and Tg mice treated with Neurotropin; FUS levels were detected by Western blot. **(G)** The interaction of Calhm2 and EFhd2 in Tg mice and Neurotropin-treated Tg mice was verified by Co-IP, n = 6. **(H)** Co-localization of Calhm2 and EFhd2 by Immunofluorescence Staining in BV-2 Cells treated with LPS, with or without Neurotropin, n=3. The expression of Calhm2 and EFhd2 in Calhm-overexpressed BV-2 cells was assessed *via* **(I)** qRT-PCR and (J) Western blot, n = 3. $^{**}p < 0.01$, $^{***}p < 0.001$.

activation, neuroinflammation, and mitochondrial dysfunction, and reduced Aβ pathology and cognitive decline in 5xFAD mice. We also revealed that Calhm2 was involved in Neurotropin-mediated effects in AD. Calhm2 overexpression attenuated the protective effects of Neurotropin against LPS-induced mitochondrial dysfunction and inflammation in microglial cells. Additionally, we found that FUS targeted Calhm2, which interacts with EFhd2. Eventually, the FUS/Calhm2 regulatory axis was validated using 5xFAD mice. Collectively, our results highlight the critical role of FUS/Calhm2 in Neurotropin-mediated microglial polarization and mitochondrial dysfunction in AD, providing a foundation for using Neurotropin as a treatment method for AD.

Mitochondrial dysfunction and microglial polarization to M1 phenotype are significant contributors to AD pathogenesis (*24*). The interaction with Aβ disrupts mitochondrial electron transfer system activity and induces the activation of M1 microglia, leading to

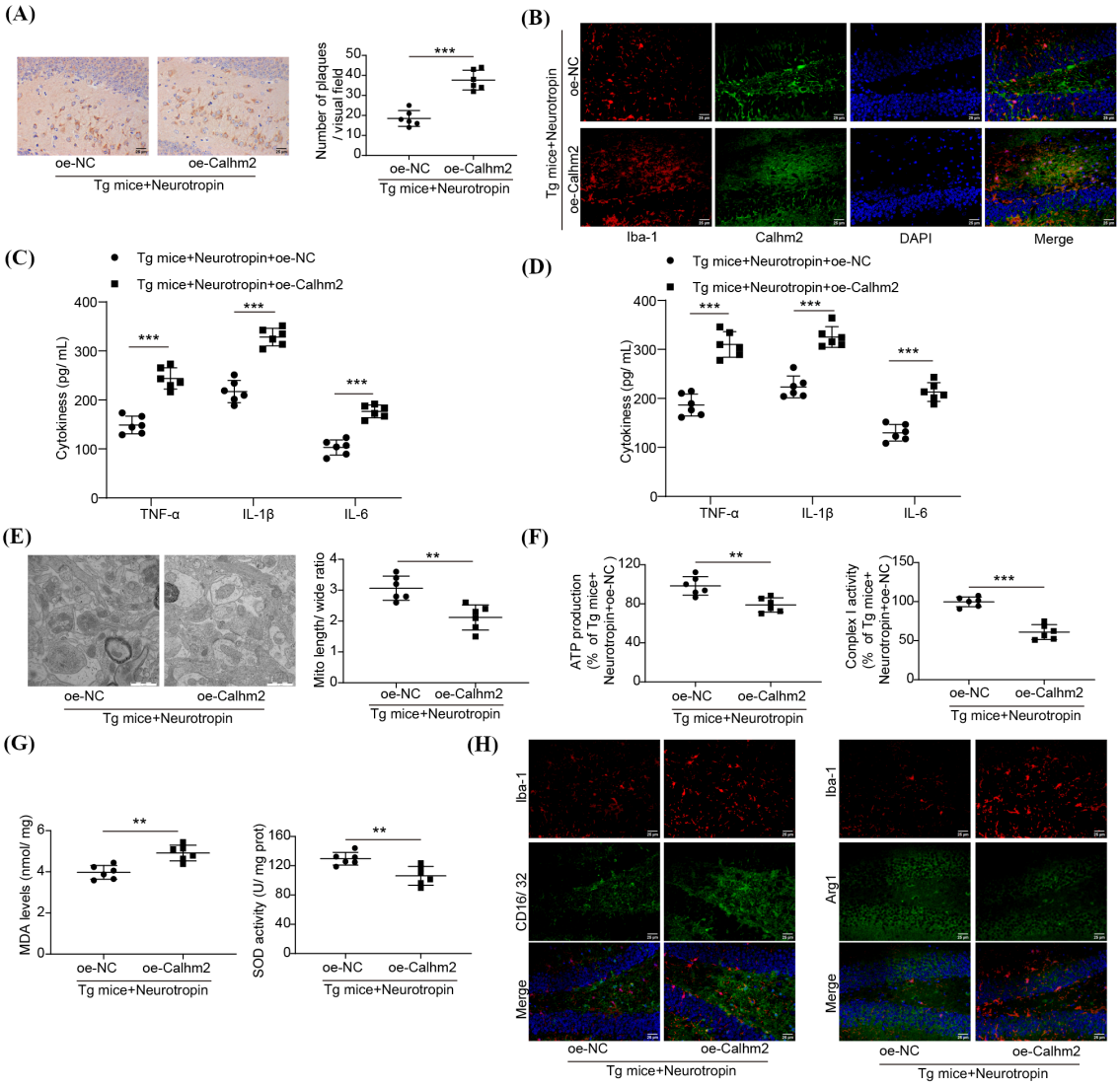

Figure 7. Neurotropin rescues brain ATP deficiency, mitochondrial dysfunction, and microglia M1 polarization *via* Calhm2 in 5xFAD mice. Neurotropin was used to treat Tg mice, and Calhm2 was overexpressed. **(A)** Immunohistochemical staining of 6E10 in the hippocampus of mice, and the number of plaques. **(B)** Co-localization of Calhm2 and Iba-1 was assessed by immunofluorescence staining. ELISA assay for measuring IL-1β, IL-6, and TNF-α in **(C)** serum and **(D)** hippocampal tissues. **(E)** Mitochondrial morphology in the hippocampus was observed by TEM. **(F)** Energy metabolism was estimated based on ATP level and respiratory chain complex I activity in the hippocampus. **(G)** MDA production and SOD activity in the hippocampus were measured. **(H)** Co-expression of Iba1 and M1/M2 polarization markers, CD16/32 for M1 and Arg1 for M2, in the hippocampal sections. $n = 6$. $^{**}p < 0.01$, $^{***}p < 0.001$.

reduced ATP production, increased ROS generation, and excretion of inflammatory cytokines (*25*). This eventually leads to aggressive AD progression (*25*). Previous studies indicated that reverse mitochondrial dysfunction and the activation of M1 microglia could attenuate AD in animal models. For instance, mitochondrial function can be restored by the stimulation of insulin signaling in AD (*26*). Another study from An *et al*. showed that exenatide decreased mitochondrial dysfunction and cognitive impairment in the 5×FAD mouse model of Alzheimer's disease (*27*). Additionally, overexpression of MKP-1 induced microglia polarized to the M2 phenotype and reduced the M1 phenotype microglia (*28*). Similar to these studies, we revealed that Neurotropin treatment attenuated the activation of microglia and neuroinflammation in 5xFAD mice and LPS-induced M1 microglial polarization. We also observed that Neurotropon treatment inhibited mitochondrial dysfunction in terms of mitochondrial morphology, mtDNA, and energy metabolism in 5xFAD mice and LPS-induced microglial cells.

Previous studies have shown that calcium homeostasis is closely related to neuroinflammation and microglial activation (*14*). The genetic knockout of calcium channels, along with specific pharmacological inhibition, has shown protective effects against AD pathology and improvements in cognitive function in AD models (*29,30*). Furthermore, blocking calcium channels with Nicardipine significantly diminished microglial activation *in vitro* (*31*). This suggests that the

Calhm family may be a potential therapeutic target for AD. Among the Calhm family members, Calhm1 did not show significant differences in 5xFAD mice and WT mice. Calhm2 and Calhm3 were significantly increased in 5xFAD mice in comparison to WT mice; however, only the expression of Calhm2 was reduced in 5xFAD mice after Neurotropin treatment. Furthermore, Calhm2 was colocalized with microglial cells, suggesting that Calhm2 might play a role in Neurotropin-mediated microglial deactivation and AD. Consistent with our data, Cheng *et al*. also documented that Calhm2 was highly expressed in the AD mouse model (*14*). Knockout of Calhm2 remarkably decreased Aβ deposition and neuroinflammation (*14*). Another recent study by Liao *et al*. demonstrated that the V136 mutation was closely correlated with AD, as it led to the loss of Calhm2 ATP release in astrocytes (*32*). Our study further demonstrated that Calhm2 overexpression reversed the inhibitory effects of Neurotropin on microglial M1 polarization, inflammatory cytokine secretion, and mitochondrial dysfunction in LPS-induced microglia, confirming that Calhm2 is associated with Neurotropin-modulated AD. To the best of our knowledge, this study revealed for the first time that Neurotropin mediates its effects on microglia *via* Calhm2.

FUS, a multifunctional RNA/DNA-binding protein, is involved in numerous cellular processes such as DNA repair, cell proliferation, transcription, and RNA and microRNA processing (*33*). Increasing evidence suggests that FUS may play a role in the pathological mechanisms of neurodegenerative diseases (*33*). The abnormal aggregation of the FUS protein has been observed in several neurodegenerative disorders, including amyotrophic lateral sclerosis (ALS), frontotemporal lobar degeneration (FTLD), and polyglutamine diseases (*34,35*). Regarding AD, it was demonstrated by a recent study that FUS was associated with the catalytic subunit of mitochondrial ATP synthase, known as ATP5B. This interaction disrupted the assembly of ATP synthase complexes and subsequently suppressed the synthesis of ATP in mitochondria (*18*). However, the role of FUS in AD was not fully understood. In our study, we found that FUS expression was increased in 5xFAD mice compared to wild-type mice, and FUS regulated the transcription of Calhm2 in microglia. This is the first report indicating the regulatory role of FUS on Calhm2. Similarly, many studies also suggest that FUS exerts these effects by binding to RNA and DNA or by regulating the transcription of downstream genes (*36*). For instance, FUS regulates critical autophagosome formation genes, including FIP200, ATG16L1, and ATG12, in a mouse neuroblastoma cell line (*35*). Another study reported that FUS modulates the transcription of the manganese superoxide dismutase gene (*37*). These further supported our conclusion that the transcription of Calhm2 was modulated by FUS in microglia.

Furthermore, our research revealed that Calhm2 interacts with EFhd2 in AD. Treatment with Neurotropin significantly reduced the binding between Calhm2 and EFhd2 in 5xFAD mice. This finding suggests that Neurotropin may regulate mitochondrial function, microglial polarization, and neuroinflammation by diminishing the interaction between Calhm2 and EFhd2. Consistently, a previous study from Bo *et al*. also documented that Calhm2 regulated STAT3 signaling in microglia by interacting with EFhd2, which resulted in enhanced microglial activation, contributing to the progression of Parkinson's disease (*38*). In addition, the depletion of EFhd2 remarkably reduced LPS-induced macrophage inflammation (*39*).

In summary, our research demonstrated that Neurotropin mitigates mitochondrial dysfunction and inhibits microglial polarization *via* the FUS/Calhm2/EFhd2 axis. These findings establish a novel theoretical foundation for using Neurotropin as a therapeutic approach for Alzheimer's disease. While our study provides valuable insights into the mechanisms by which Neurotropin alleviates AD pathology, several limitations should be considered. First, the research primarily utilized the 5xFAD mouse model, which may not fully replicate the complexity of human AD. Consequently, further studies involving diverse animal models and human subjects are necessary to validate these findings. Second, past research has shown that under physiological conditions, FUS is primarily located in the nucleus. However, during neurodegenerative diseases, FUS translocates to the cytoplasm. Due to funding restrictions, we did not examine whether FUS translocates to the cytoplasm in LPS-induced microglia. Investigating this phenomenon would be an interesting direction for future research. Finally, although we observed significantly elevated levels of IL-1β, IL-6, and TNF-α in both the hippocampus and serum of Calhm2-overexpressing mice, we did not directly evaluate blood–brain barrier (BBB) integrity, which may contribute to this phenomenon. Direct assessment of BBB function should therefore be included in future work.

Funding: This work was supported by the National Natural Science Foundation of China (No. 82360244).

Conflict of Interest: The authors have no conflicts of interest to disclose.

Ethics approval and consent to participate: This research was conducted in strict accordance with the ARRIVE guidelines. The study protocol was thoroughly evaluated and received approval from the Ethics Committee of The First Affiliated Hospital of Nanchang University (Approval No. CDYFY-IACUC-202401QR002).

Availability of data and material: All data generated or analyzed during this study are included in this published article.

References

1. Vejandla B, Savani S, Appalaneni R, Veeravalli RS, Gude SS. Alzheimer's Disease: The Past, Present, and Future of a Globally Progressive Disease. Cureus. 2024; 16:e51705.
2. Li X, Feng X, Sun X, Hou N, Han F, Liu Y. Global, regional, and national burden of Alzheimer's disease and other dementias, 1990-2019. Front Aging Neurosci. 2022; 14:937486.
3. GBD 2019 Dementia Forecasting Collaborators. Estimation of the global prevalence of dementia in 2019 and forecasted prevalence in 2050: an analysis for the Global Burden of Disease Study 2019. Lancet Public Health. 2022; 7:e105-e125.
4. Knopman DS, Amieva H, Petersen RC, Chételat G, Holtzman DM, Hyman BT, Nixon RA, Jones DT. Alzheimer disease. Nat Rev Dis Primers. 2021; 7:33.
5. Hampel H, Hardy J, Blennow K, Chen C, Perry G, Kim SH, Villemagne VL, Aisen P, Vendruscolo M, Iwatsubo T, Masters CL, Cho M, Lannfelt L, Cummings JL, Vergallo A. The Amyloid-β Pathway in Alzheimer's Disease. Mol Psychiatry. 2021; 26:5481-5503.
6. Zhang H, Wei W, Zhao M, Ma L, Jiang X, Pei H, Cao Y, Li H. Interaction between Aβ and Tau in the Pathogenesis of Alzheimer's Disease. Int J Biol Sci. 2021; 17:2181-2192.
7. Toda K, Muneshige H, Ikuta Y. Antinociceptive effects of neurotropin in a rat model of painful peripheral mononeuropathy. Life Sci. 1998; 62:913-921.
8. Fang W, Liao W, Zheng Y, Huang X, Weng X, Fan S, Chen X, Zhang X, Chen J, Xiao S, Thea A, Luan P, Liu J. Neurotropin reduces memory impairment and neuroinflammation *via* BDNF/NF-κB in a transgenic mouse model of Alzheimer's disease. Am J Transl Res. 2019; 11:1541-1554.
9. Miao J, Ma H, Yang Y, Liao Y, Lin C, Zheng J, Yu M, Lan J. Microglia in Alzheimer's disease: pathogenesis, mechanisms, and therapeutic potentials. Front Aging Neurosci. 2023; 15:1201982.
10. Guo S, Wang H, Yin Y. Microglia Polarization From M1 to M2 in Neurodegenerative Diseases. Front Aging Neurosci. 2022; 14:815347.
11. Wang C, Zong S, Cui X, Wang X, Wu S, Wang L, Liu Y, Lu Z. The effects of microglia-associated neuroinflammation on Alzheimer's disease. Front Immunol. 2023; 14:1117172.
12. Hansen DV, Hanson JE, Sheng M. Microglia in Alzheimer's disease. J Cell Biol. 2018; 217:459-472.
13. Agrawal I, Jha S. Mitochondrial Dysfunction and Alzheimer's Disease: Role of Microglia. Front Aging Neurosci. 2020; 12:252.
14. Cheng J, Dong Y, Ma J, Pan R, Liao Y, Kong X, Li X, Li S, Chen P, Wang L, Yu Y, Yuan Z. Microglial Calhm2 regulates neuroinflammation and contributes to Alzheimer's disease pathology. Sci Adv. 2021; 7:eabe3600.
15. Rubio-Moscardo F, Setó-Salvia N, Pera M, *et al*. Rare variants in calcium homeostasis modulator 1 (CALHM1) found in early onset Alzheimer's disease patients alter calcium homeostasis. PLoS One. 2013; 8:e74203.
16. Mun MJ, Kim JH, Choi JY, Jang WC. Calcium homeostasis modulator 1 gene P86L polymorphism and the risk for alzheimer's disease: A meta-analysis. Neurosci Lett. 2016; 619:8-14.
17. Ma Z, Taruno A, Ohmoto M, *et al*. CALHM3 Is Essential for Rapid Ion Channel-Mediated Purinergic Neurotransmission of GPCR-Mediated Tastes. Neuron. 2018; 98:547-561.e10.
18. Deng J, Wang P, Chen X, Cheng H, Liu J, Fushimi K, Zhu L, Wu JY. FUS interacts with ATP synthase beta subunit and induces mitochondrial unfolded protein response in cellular and animal models. Proc Natl Acad Sci U S A. 2018; 115:E9678-E9686.
19. Sahadevan S, Hembach KM, Tantardini E, Pérez-Berlanga M, Hruska-Plochan M, Megat S, Weber J, Schwarz P, Dupuis L, Robinson MD, De Rossi P, Polymenidou M. Synaptic FUS accumulation triggers early misregulation of synaptic RNAs in a mouse model of ALS. Nat Commun. 2021; 12:3027.
20. Jiang T, Tan L, Zhu XC, Zhang QQ, Cao L, Tan MS, Gu LZ, Wang HF, Ding ZZ, Zhang YD, Yu JT. Upregulation of TREM2 ameliorates neuropathology and rescues spatial cognitive impairment in a transgenic mouse model of Alzheimer's disease. Neuropsychopharmacology. 2014; 39:2949-2962.
21. Bhatia S, Rawal R, Sharma P, Singh T, Singh M, Singh V. Mitochondrial Dysfunction in Alzheimer's Disease: Opportunities for Drug Development. Curr Neuropharmacol. 2022; 20:675-692.
22. Ishikawa T, Yasuda S, Minoda S, Ibuki T, Fukuhara K, Iwanaga Y, Ariyoshi T, Sasaki H. Neurotropin® ameliorates chronic pain *via* induction of brain-derived neurotrophic factor. Cell Mol Neurobiol. 2015; 35:231-241.
23. Mutoh T, Yamamoto S, Moriya T. Correction: Mutoh *et al*. Post-Event Application of Neurotropin Protects against Ischemic Insult toward Better Outcomes in a Murine Model of Subarachnoid Hemorrhage. Biomedicines 2021, 9, 664. Biomedicines. 2024; 12:2033.
24. Wu YG, Song LJ, Yin LJ, Yin JJ, Wang Q, Yu JZ, Xiao BG, Ma CG. The effects and potential of microglial polarization and crosstalk with other cells of the central nervous system in the treatment of Alzheimer's disease. Neural Regen Res. 2023; 18:947-954.
25. Misrani A, Tabassum S, Yang L. Mitochondrial Dysfunction and Oxidative Stress in Alzheimer's Disease. Front Aging Neurosci. 2021; 13:617588.
26. Potenza MA, Sgarra L, Desantis V, Nacci C, Montagnani M. Diabetes and Alzheimer's Disease: Might Mitochondrial Dysfunction Help Deciphering the Common Path? Antioxidants (Basel). 2021; 10:1257.
27. An J, Zhou Y, Zhang M, Xie Y, Ke S, Liu L, Pan X, Chen Z. Exenatide alleviates mitochondrial dysfunction and cognitive impairment in the 5×FAD mouse model of Alzheimer's disease. Behav Brain Res. 2019; 370:111932.
28. Li J, Wang L, Zeng Q, He J, Tang Q, Wang K, He G. MKP-1 regulates the inflammatory activation of microglia against Alzheimer's disease. CNS Neurosci Ther. 2024; 30:e14409.
29. Goodison WV, Frisardi V, Kehoe PG. Calcium channel blockers and Alzheimer's disease: potential relevance in treatment strategies of metabolic syndrome. J Alzheimers Dis. 2012; 30 Suppl 2:S269-282.
30. Tan Y, Deng Y, Qing H. Calcium channel blockers and Alzheimer's disease. Neural Regen Res. 2012; 7:137-140.
31. Huang BR, Chang PC, Yeh WL, Lee CH, Tsai CF, Lin C, Lin HY, Liu YS, Wu CY, Ko PY, Huang SS, Hsu HC, Lu DY. Anti-neuroinflammatory effects of the calcium channel blocker nicardipine on microglial cells: implications for neuroprotection. PLoS One. 2014;

9:e91167.
32. Liao Y, Wang Y, Tao QQ, Yang C, Wang J, Cheng J, Ma J, Wu ZY, Pan RY, Yuan Z. CALHM2 V136G polymorphism reduces astrocytic ATP release and is associated with depressive symptoms and Alzheimer's disease risk. Alzheimers Dement. 2023; 19:4407-4420.
33. Deng H, Gao K, Jankovic J. The role of FUS gene variants in neurodegenerative diseases. Nat Rev Neurol. 2014; 10:337-348.
34. Woulfe J, Gray DA, Mackenzie IR. FUS-immunoreactive intranuclear inclusions in neurodegenerative disease. Brain Pathol. 2010; 20:589-597.
35. Doi H, Koyano S, Suzuki Y, Nukina N, Kuroiwa Y. The RNA-binding protein FUS/TLS is a common aggregate-interacting protein in polyglutamine diseases. Neurosci Res. 2010; 66:131-133.
36. Ishigaki S, Masuda A, Fujioka Y, Iguchi Y, Katsuno M, Shibata A, Urano F, Sobue G, Ohno K. Position-dependent FUS-RNA interactions regulate alternative splicing events and transcriptions. Sci Rep. 2012; 2:529.
37. Dhar SK, Zhang J, Gal J, Xu Y, Miao L, Lynn BC, Zhu H, Kasarskis EJ, St Clair DK. FUsed in sarcoma is a novel regulator of manganese superoxide dismutase gene transcription. Antioxid Redox Signal. 2014; 20:1550-1566.
38. Bo X, Xie F, Zhang J, Gu R, Li X, Li S, Yuan Z, Cheng J. Deletion of Calhm2 alleviates MPTP-induced Parkinson's disease pathology by inhibiting EFHD2-STAT3 signaling in microglia. Theranostics. 2023; 13:1809-1822.
39. Tu Y, Zhang L, Tong L, Wang Y, Zhang S, Wang R, Li L, Wang Z. EFhd2/swiprosin-1 regulates LPS-induced macrophage recruitment *via* enhancing actin polymerization and cell migration. Int Immunopharmacol. 2018; 55:263-271.

Received July 24, 2025; Revised August 25, 2025; Accepted September 18, 2025.

**Address correspondence to:*
Lingling Ye, Department of Anesthesiology and Operative Medicine, Medical Center of Anesthesiology and Pain, The First Affiliated Hospital Of Nanchang University, No. 17, Yongwaizheng Street, Nanchang 330006, Jiangxi Province, China.
E-mail: ndyfy03678@ncu.edu.cn

Released online in J-STAGE as advance publication September 26, 2025.